

Detection of Oil Spills in SAR Images using Threshold Segmentation Algorithms

Alaa Sheta
Taif University
Taif, Saudi Arabia

Mouhammd Alkasasbeh
Mutah University
Jordan

Malik Braik
University of Birmingham
Birmingham, Edgbaston, UK

Hafsa Abu Ayyash
Al-Balqa Applied University
Salt, Jordan

ABSTRACT

Identification of potential oil spills on Synthetic Aperture Radar (SAR) satellite images is a complex process. Oil companies, as well as the coast guard have tested a whole range of methods for monitoring and detection of possible oil spills. These methods are found to be expensive, complex and require high processing power and time. In this paper, an oil spill detection method is proposed. The method consists of four main stages, namely: 1) Image enhancement; 2) Image segmentation 3) feature extraction; and 4) Object recognition of the segmented objects as oil spills or look-alikes. The algorithm was trained on a large number of Synthetic Aperture Radar (SAR) images. The proposed thresholding algorithm can be considered an alternative to manual inspection for large ocean areas. Promising results and high detection rates for the oil spills have been achieved.

General Terms:

Image Processing, Object Recognition

Keywords:

Oil Spill Detection, Thesholding, Segmentationifx

1. INTRODUCTION

Petroleum production has been an essential component for the modern industry. Oil is needed in diversity of industrial processes. Oil has to be transported in seas and oceans. During transportation, oil spills can happen. The major sources of oil spill pollution are mainly due to: Tanker accidents or ballast water. Once oil is spilled, it quickly spreads to form a thin layer on the water surface, known as an "oil slick". Marine oil spill is highly dangerous because of many environmental factors. It can be easily spread over a wide area [10]. Between 1988 and 2000, there were 2,475 spills, which released over 800,000 liters of oil in Toronto and surrounding regions [12]. Over the years, many methods for monitoring and detecting of possible oil spills were tested. Some of these methods include: Infra-Red (IR) radiation, radar, lasers and many types of night-vision schemes. Unluckily, these methods are found to be both expensive, complex and require high processing power and time. Nevertheless, they fail to provide promising solutions [2, 13]. Consequently, it is a must to have an efficient technique for monitoring and detecting oil spills. Aircraft and ship-based sensors are not fully adequate for sea monitoring and oil spill detection. This is due to the limited coverage and the operational costs [19]. Table 1 shows the largest and recent oil spill in the world [15], containing the Ship/Incident, location, date of the accident and the quantity of spilled oil in tones.

Table 1. Largest and recent oil spill [15]

Ship/Incident	Location	Date	Tones
Gulf War	Sea Island, Kuwait	Nov 26,91	800000
IxtoC/blowout	Gulf of Mexico, Mexico	Jun 06,79	470000
Atlantic Empress	Caribbean Sea, off Tobago	Jul 19, 79	300000
Castillo de Bellver	Saldanha Bay, South Africa	Aug 08,83	260000
Amoco Cadiz	Coast of Brittany, France	Mar 06,78	235000
Exxon Valdez	Prince William Sound	Mar 24,89	39000
Aegean Sea	La Coruna, Spain	Dec 05,92	75000
Erika	Coast of Brittany	Dec 12,99	10000
Prestige	Coast of Galisia, Spain	Nov 19,02	40000

1.1 SAR Images

Nowadays, with the advent of remote-sensing techniques solving oil spill detection and monitoring problems using SAR images became very promising [1]. Satellite-borne SAR provides a number of advantages compared to other systems for the detection and monitoring process of oil spills. The SAR images can include almost everything on the earth specifically seas and oceans, no matter of the weather conditions, if it's windy or cloudy. And it has the capability to take images during the day and the nights also. The SAR images have the ability to detect and distinction between the objects on the sea like it is ships or sea animals or even the oil spills. Most important here in the SAR images is the variance between the foreground and the background of the image itself. The SAR images by itself have difficulties to be fully automatic oil spill's detection system, so that other add-in needed to complete its work [2]. A fully automated system for the identification of possible oil spills presented on Synthetic Aperture Radar (SAR) satellite images based on fuzzy logic was presented in [11]. The developed system analyzes the satellite images and assigns the probability of a dark image shape to be an oil spill for Aegean Sea in Greece.

The rest of this paper is organized as follows: Section 2 briefly summarizes the main steps in the proposed algorithm, also it provides a flowchart which illustrates each phase of the proposed technique. In Section 3, we describe the image enhancement phase in details; it consists of contrast stretching and Gaussian filtering. Section 4 introduces the detailed procedure of the detection phase, and the achieved results for each step. Moreover, four successive steps are combined successively to accomplish this phase; they are: local thresholding, land masking, global thresholding and merging. The spot feature extraction phase is presented in Section 5. Then; we illustrate the spot classification algorithm in Section 6. Finally, Section 7 contains concluding and future work remarks.

2. PROPOSED THRESHOLDING ALGORITHM

This work focuses on the segmentation and characterization of oil slicks in the marine environment using Synthetic Aperture Radar (SAR) images. The proposed segmentation algorithm is

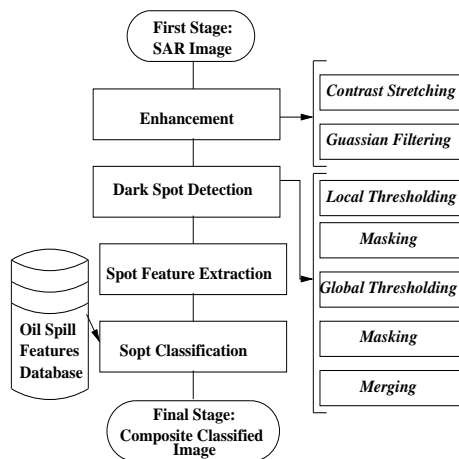


Fig. 1. Proposed Oil Spill Detection Algorithms

based on local and global threshold techniques, while the classification process is implemented in a set of extracted features presented in [2, 4] and fully utilized based on statistical features in the oil spill domain.

The main approach which is used to detect the dark spots, consists of local and global threshold techniques. For each dark spot, a number of features have been counted in order to classify the slick as either an oil slick or other possible objects in the sea. The proposed approach detects the dark spots in the images primarily using local and global threshold techniques [2, 4]. For each dark spot, a number of features are expressed in order to classify the slick as either an oil slick or a look alike [4]. The proposed threshold algorithm, initially analyzes the SAR images, and then assigns a probability to the dark spot to indicate whether it is an oil spill or look alike.

The entire stages of the proposed algorithm are shown in Figure 1. The algorithm consists of four main phases:

- (1) A preprocessing phase which consists of traditional image enhancement methods.
- (2) A threshold segmentation algorithm for the detection of possible oil spills.
- (3) For each dark spot, a set of features is calculated to classify the slick as either oil slick or look alike.
- (4) Finally, a classification criterion is carried out, which separates oil spills from look alikes. A classification scheme is utilized based on statistical features using the oil spill features database.

3. IMAGE ENHANCEMENT

Reducing the noise and smoothing the image are the most critical steps before applying the segmentation process. Consequently, the natural variations and noise inside the SAR images will disturb the segmentation process, which in turn leads to the quality of the segmented images which based on the type of filter that had been used. Adaptive filters based on appropriate scene and speckle model are the most fitting filters for SAR images [18, 16].

In addition, the enhancement methods also used to improve the visual appearance of SAR images in order to obtain the best possible image perception. This can be accomplished by sharpening the image features and increasing the contrast of the image [7]. This preprocessing phase must manage the effects of noise and increases the visibility of the image [8]. Moreover, artificial neural network was used to enhance SAR images [21]. Furthermore, in the work of [22], an adaptive image enhancement method based on Contourlet transform was used to improve the

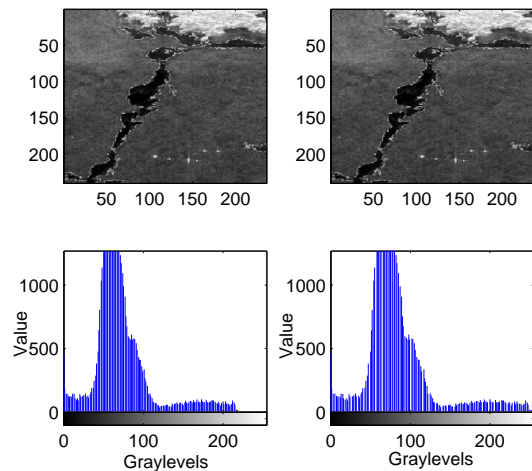


Fig. 2. Upper Left: Input image, Upper right: Contrast stretching image, Lower left: Original histogram, Lower right: Contrast stretching histogram

quality of the images. The author claimed that their results provided a significant performance even with low contrast.

3.1 Contrast Stretching

Low-contrast images may result from different factors, for example, the poor illumination of the camera, or the absence of dynamic range in the imaging sensor, or even wrong setting of lens aperture during image acquisition. Contrast stretching is one of the simplest piecewise linear functions [3]. Contrast stretching technique improves the readability of low contrast areas in the SAR image. Figure 2 shows the effect of contrast stretching technique on the SAR image. It can be seen from Figure 2 that the contrast stretching process has two effects:

- (1) Increase the dynamic range of the gray levels within the image being processed by contrast stretching.
- (2) Increase the histogram of the overall intensity of the processed image, so that the new image appears more obvious than the original SAR image. Also, the processed image histogram is distributed over a large range when it's compared to the histogram of the original SAR image.

3.2 Gaussian Filtering

Gaussian filter is proposed for removing the noise as it preserves the structural and textural features, and also can improve the image quality for better estimation [18]. Speckles can be reduced, in the intensity images, using the moving kernel which has the shape of the Gaussian hump. The moving window size of the filter is selected as (41×41) . The Gaussian filter is defined as given in Equation 1 [8]:

$$G(x, y) = \frac{1}{2\pi\sigma^2} e^{-\frac{x^2+y^2}{2\sigma^2}} \quad (1)$$

where σ is the standard deviation of the distribution, x and y are the directions of the kernel. The SAR image produced from the contrast stretching phase is passed to the Gaussian filter. The result of applying Gaussian filter to the stretched image is shown in Figure 3. It is recognizable that the quality of the image compared to the stretched image is improved. Additionally, the dark slicks appeared sharp and their shapes are retained. The histogram of the filtered image is not fully distributed over a wide range as in contrast stretching technique; this is because

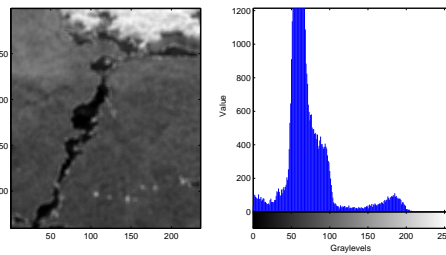


Fig. 3. Filtered using Gaussian filter, Right: Histogram of the filtered image



Fig. 4. Local threshold segmented image

the Gaussian filter removes the noise while preserving the details and edges. Consequently, the image enhancement step illustrates the differences between the oil spill objects and the background.

4. DARK SPOT DETECTION

The dark spot detection locates all spots in the SAR image, which represents oil slicks. The oil spills are mainly characterized by their dark levels with respect to the background. Many phases are developed and add up for the dark spot detection module as given in the following subsections.

4.1 Local Threshold

It computes a set of low spots in the SAR image to find the borders between the oil slick and the surrounding sea [20]. Local threshold segments the image into two classes:

- (1) Class 1: which has the pixels below a predefined threshold value, and
- (2) Class 2: which has the pixels above the same threshold value.

This operation is applied to each individual pixel on a local level by computing the local mean value in a window which moves across the image. Figure 4 shows the result of local threshold technique when applied to the smoothed SAR image. The window size in this work is eight connected neighborhood. Although the dark spots are not accurately segmented, the following stages of spot detection are needed in order to complete the detection process.

4.2 Land Masking

Land regions involve several dark regions, which may deceive the classification process. This is why; the land mask is an important stage in dark spot detection. Land masking process [17]

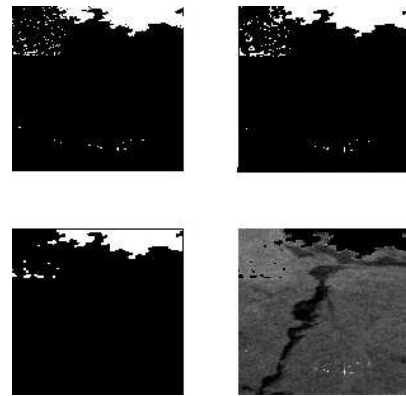


Fig. 5. Upper left: Binary image, Upper right: Closing the image, Lower left: Opening the resulted image, Lower right: The segmented image

can reduce or may eliminate the dark regions in the image by following the three steps just as given below:

- (1) Convert the image to binary using a predefined thresholding level. In this work, the level selected is to be 0.5.
- (2) The output binary image has two values 0 (black) for all pixels in the input image with luminance less than 0.5, and 1 (white) for all other pixels.
- (3) Apply a morphological filter with closing and opening operations.

Morphological operations are ways of extracting image elements like regions, shape, boundaries and so on. A detailed explanation of mathematical morphology operations can be found in [8]. Dilation and erosion are the two basic morphological operations. The Structure element (S) used in this stage has a size of 3×3 as shown in the following matrix:

$$S = \begin{bmatrix} 0 & 1 & 0 \\ 1 & 1 & 1 \\ 0 & 1 & 0 \end{bmatrix} \quad (2)$$

S is a matrix that defines a neighborhood shape and size for morphological operations consisting of only 0's and 1's. S has an arbitrary shape and size. The pixels with values of 1 define the neighborhood. The results of applying land masking filter are shown in Figure 5.

4.3 Global Thresholding

The first step in the global threshold is to get the image complement, so that the zeros become ones and the ones become zeros; i.e. black and white are reversed. The window addressed at this stage is the entire image. All pixels corresponding to the digital number values less than the threshold value are registered as pixels of dark regions.

The global image threshold value is computed using Otsu's method. This method can be used to convert the input intensity image to a binary image [5, 9]. The level is a normalized intensity value that lies within the range of $[0, 1]$. The Otsu's method determines the threshold value to minimize the intra class variance of the threshold black and white pixels. The result of global threshold stage is shown in Figure 6. As seen in Figure 6, some tiny gaps are resulted from applying the global threshold. These small gaps can be removed using the following sequential operations: the dilation operator is applied to bridge these gaps using



Fig. 6. Global segmented image

the defined S in the previous stage. Then, the opening operator using the same S is applied to smooth the contour of the lands' objects. In sum, tiny protrusions are eliminated from the image.

4.4 Merging

Merging is the finishing stage in the spot detection algorithm. The final spot image is constructed by combining the two images resulted from the land masking and global threshold stages. The segmented objects were controlled over the spot detection problem without losing any small objects in the image. The final segmented image is shown in Figure 6. It can be seen that the proposed algorithm produces the best segmentation of the dark areas, this image includes only the oil spills, which can be used as a prior task to posterior classification.

5. SPOT FEATURE EXTRACTION

Classification accuracies are highly dependent on the feature set selection. In other words, classification accuracy is as good as the feature set that is selected to represent an image. For each dark spot, a set of features are calculated [6]. The dark spots are then classified into either probably oil slicks or other objects based on the extracted features. The extracted features are defined as follows:

- (1) The Area of the segmented object represents the number of pixels in the object.
- (2) The Max of the segmented object indicates the pixel of the largest value in the object.
- (3) Entropy (e) is a measure of randomness [8]. The entropy is defined as given in Equation 3.

$$e = - \sum_{i=0}^{L-1} p(z_i) \log_2 p(z_i) \quad (3)$$

where z_i is the image intensity, $p(z)$ is the histogram of the intensity levels in a region, and L is the number of possible intensity levels.

- (4) Uniformity (U) is also known as Energy, uniformity of energy, or angular second moment. Uniformity measures the maximum gray level when they are equal. The uniformity is defined as given in Equation 4 [8].

$$U = \sum_{i=0}^{L-1} p^2(z_i) \quad (4)$$



Fig. 7. Final segmented image

- (5) Mean (m) measures the average intensity [8]. Mean is defined as given in Equation 5.

$$m = \sum_{i=0}^{L-1} z_i p(z_i) \quad (5)$$

- (6) Standard Deviation (σ) measures the average contrast [8]. Standard deviation is defined as given in Equation 6.

$$\sigma = \sqrt{z_i - m^2} = \sqrt{\sigma^2} \quad (6)$$

- (7) Skewness (μ_3) is known as Third moment, it measures the third order moment about the mean. Skewness is defined as given in Equation 7 [8].

$$\mu_3 = \sum_{i=0}^{L-1} (z_i - m)^3 p(z_i) \quad (7)$$

- (8) Smoothness (R) measures the relative's smoothness of the intensity in the region [8]. Smoothness is defined as given in Equation 8.

$$R = 1 - 1/(1 + \sigma^2) \quad (8)$$

6. SPOT CLASSIFICATION

Herein, is the final stage of the proposed method, where each segmented object is recognized as an oil spill object or not. This stage helps reducing the false alarm which may be acquired. A group of features have been used as evaluation criteria to detect the type of each object. These features have been tested for a group of segmented oil spill objects. The true locations of the oil spill objects were defined in [7]. In Table 2, its shown the values of each feature of the intensity values of each segmented object. It was found that each feature on the oil spill object has a specific range of intensity values. The range of each feature value and the true location of oil spill objects are compared to the values given in [7]. This range is called an *oil spill domain*. The extracted features of the oil spill objects were tested based on the true domain. The intensity values of the extracted features are found within the true range as shown in Table 3. Consequently, each feature of the segmented object located within the true range is classified as an oil spill; all other looks alike objects are located out of the true range. The proposed method was able to validate whether a slick is oil spot or something similar. The segmented image shown in Figure 7 contains only oil spills. Furthermore, all slicks with feature values located

Table 2. Feature intensity values for a group of segmented oil spill objects

Object No.	Area	Max	Entropy	Uniformity	Skewness	Smoothness	Std	Mean
1	355	129	5.24	0.1	0.6008	0.0163	32.92	28.76
2	455	129	4.4733	0.19	0.623	0.014	30.4	21.32
3	13318	107	4.688	0.05	0.0306	0.005	18.11	23.66
4	436	131	5.096	0.04	0.3857	0.0129	29.22	34.25
5	1145	75	4.4564	0.049	-0.004	0.0024	12.45	52.21
6	4463	69	4.3693	0.053	-0.0073	0.0019	11.26	46.14
7	632	69	4.3467	0.059	-0.0153	0.0022	11.88	38.88
8	24402	155	4.66	0.07	0.05	0.0058	19.5	22.76
9	1523	73	4.7587	0.04	-0.0348	0.0034	14.82	35.49
10	922	70	4.7905	0.04	-0.0211	0.0031	14.16	35
11	1621	100	3.4009	0.28	0.1167	0.0058	19.45	14.66
12	464	73	4.3137	0.11	0.053	0.0062	20.2	21.65
13	1016	64	4.4412	0.057	-0.0319	0.0024	12.49	41.76
14	552	79	4.79	0.04	-0.0115	0.003	13.88	36.08
15	417	79	4.8664	0.04	0.0033	0.0033	14.61	34.68
16	1023	185	4.9425	0.04	0.0982	0.0046	17.32	30.4
17	1573	87	4.6478	0.05	-0.0091	0.0023	12.14	36.74
18	1371	77	4.6602	0.05	-0.0029	0.0023	12.12	37.96
19	775	85	4.647	0.05	0.0027	0.0023	12.22	39.97
20	342	91	4.6194	0.05	0.0108	0.0025	12.77	41.35
21	841	75	4.357	0.06	-0.0182	0.0019	11	56.86
22	35	52	3.1476	0.21	0.0607	0.0047	17.87	15.17
23	73	133	2.7896	0.37	1.5748	0.0272	42.91	27.14

Table 3. Extracted features domain

Feature Name	Oil Spill Domain
Area	(>=35 pixels)
Max	(52 - 185) pixels
Entropy	(2.79 - 5.24)
Uniformity	(0.04 - 0.37)
Skewness	(-0.0348 - 1.5748)
Smoothness	(0.0019 - 0.0272)
Standard Deviation	(11.00 - 42.91)
Mean	(14.66 - 56.86)

inside the true domain are classified as oil slick. In particular, the oil slicks with feature values out of the true domain are classified as look alike. In sum, the developed algorithm achieved a high accuracy in true locating of oil spills. Figure 8 shows the precise location, and the distribution of the major detected and identified oil slicks of SAR image. Comparing the segmented image in Figure 7 to the precise location of oil slicks in Figure 8, in this work, it has been found that the proposed method identifies the location of oil spills in the image accurately. Hence, persuasive results and acceptable detection rates are obtained.

7. CONCLUSION AND FUTURE WORKS

An oil spill detection algorithm was implemented based synthetic aperture radar images; this algorithm is mainly based on local and global threshold techniques. The presented algorithm can distinguish between oil spills and look alike. Oil spill classification accuracies were highly dependent on the feature set selection. The experimental results demonstrate that the proposed segmentation algorithm has the ability to detect oil spills. For future works, speeding up the computation process by using parallel programming will be taken under consideration. Moreover, another extension of this work will focus on using artificial neural network as a classifier tool instead of using a firmly established domain.

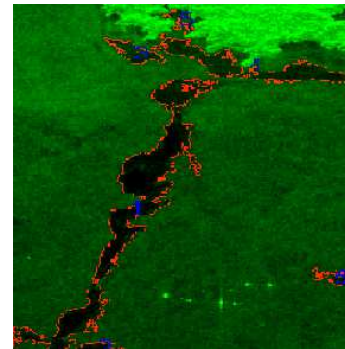


Fig. 8. True location of oil spill in SAR image of the Prestige tanker oil slick near Galicia [14]

8. ACKNOWLEDGEMENTS

Prof. Alaa Sheta is a full-time faculty member with the Computers and Systems Department, Electronics Research Institute (ERI), Cairo, Egypt. He would like to acknowledge ERI.

9. REFERENCES

- [1] Hafssa A. AbuAyyash. Improving oil spill detection using remote sensing techniques, m.sc. of computer science.
- [2] Régia T. S. Araújo, Fátima N. S. de Medeiros, Rodrigo C. S. Costa, Régis C. P. Marques, Rafael B. Moreira, and Jilseph L. Silva. Locating oil spill in SAR images using wavelets and region growing. In *IEA/AIE'2004: Proceedings of the 17th international conference on Innovations in applied artificial intelligence*, pages 1184–1193. Springer Springer Verlag Inc, 2004.
- [3] Malik Braik, Alaa Sheta, and Aladdin Ayesh. Particle swarm optimisation enhancement approach for improving

- image quality. *Int. J. Innovative Computing and Applications*, 1(2):138–145, 2007.
- [4] Lena Chang, Z. S. Tang, S. H. Chang, and Yang-Lang Chang. A region-based GLRT detection of oil spills in SAR images. *Pattern Recogn. Lett.*, 29(14):1915–1923, 2008.
- [5] I. El-Feghi, N. Adem, M. A. Sid-Ahmed, and M. Ahmadi. Improved co-occurrence matrix as a feature space for relative entropy-based image thresholding. In *Proceedings of IEEE Computer Society*, pages 314–320. Computer Graphics, Imaging and Visualisation, 2007.
- [6] F. D. Frate, A. Petrocchi, J. Lichtenegger, and G. Calabresi. Neural networks for oil spill detection using ERS SAR data. *IEEE Transaction Geosc. Rem. Sens.*, 38:2282–2287, 2000.
- [7] S. Galicia. *Galicia (Spain), November 2002-April 2003*. current URL is <http://earth.esa.int/ew/oil/slicks/galicia>, 2008.
- [8] R. Gonzalez and R. Woods. *Digital Image Processing*. Prentice Hall, 3rd Edition, 2008.
- [9] R. Gonzalez, R. Woods, and S. Eddins. *Digital Image Processing using MATLAB*. Prentice Hall, 2nd Edition, Upper Saddle River, NJ, 2004.
- [10] M. Jha, J. Levy, and Y. Gao. Advanced in remote sensing for oil spill disaster management: State of the art sensors technology for oil spill surveillance. *Sensors Journal*, 8(13):236 – 255, 2008.
- [11] Iphigenia Keramitsoglou, Constantinos Cartalis, and Chris T. Kiranoudis. Automatic identification of oil spills on satellite images. *Environ. Model. Softw.*, 21(5):640–652, May 2006.
- [12] J. Li. Spill management for the toronto AOC. Technical report, 2002.
- [13] Lin Li, Susan L. Ustin, and Mui Lay. Application of AVIRIS data in detection of oil-induced vegetation stress and cover change at jornada, new mexico. *Remote Sensing of Environment*, 94(1):1–16, January 2005.
- [14] A. Montali, G. Giacinto, M. Migliaccio, and A. Gambardella. Supervised pattern classification techniques for oil spill classification in SAR images: Preliminary results. In *European Space Agency*, pages 123–127. Advances in SAR Oceanography from Envisat and ERS Missions, 2006.
- [15] J.C. Prados. Chemical dispersants and bioremediation for the treatment of oil spills. Technical report, 2003.
- [16] A. Solberg, C. Brekke, E. Volden, and P. Husoy. Oil spill detection in radarsat and envisat SAR images. *IEEE Transactions on Geoscience and remote Sensing*, 45(3):746–755, 2007.
- [17] A. Solberg, T. Dokken, and R. Solberg. Automatic detection of oil spills in envisat, radarsat and ERS SAR images. *IEEE Geoscience and Remote Sensing Symposium*, 4(3):2747–2749, 2003.
- [18] A. H. Solberg, G. Stovrik, R. Solberg, and E. Volden. Automatic detection of oil spills in ERS SAR images. In *IEEE Transactions on Geoscience and Remote Sensing*, volume 37, pages 1916 – 1924, 1999.
- [19] Konstantinos Topouzelis, Karathanassi Vassilia, Pavlakis Petros, and Rokos Demetrius. Potentiality of feed-forward neural networks for classifying dark formations to oil spills and look-alikes. *Geocarto International*, 24(3):179–191, 2009.
- [20] Y. Tsai. A new approach for image thresholding under uneven lighting conditions. In *Proceedings of the IEEE/ACIS International Conference on Computer and Information Science, 11-13 July*, pages 123 – 127. Computer and Information Science, 2007.
- [21] V. Turkar. Polarimetric sar image classification by using artificial neural network. In *Proceedings of the International Conference and Workshop on Emerging Trends in Technology, ICWET '10*, pages 48–52, New York, NY, USA, 2010. ACM.
- [22] Ying Yu, Bin Wang, and Liming Zhang. Hebbian-based neural networks for bottom-up visual attention and its applications to ship detection in SAR images. *Neurocomput.*, 74(11):2008–2017, May 2011.